

# No evidence of histology subtype-specific prognostic signatures among lung adenocarcinoma and squamous cell carcinoma patients at early stages.

Suyan Tian<sup>1</sup><sup>§</sup>, Chi Wang<sup>2</sup>, Ming-Wen An<sup>3</sup>

<sup>1</sup>Division of Clinical Epidemiology, First Hospital of Jilin University, 71Xinmin Street, Changchun, Jilin, China, 130021

<sup>2</sup>Department of Biostatistics and Markey Cancer Center, University of Kentucky, 800 Rose St., Lexington, KY, USA, 40536.

<sup>3</sup>Department of Mathematics, Vassar College, Poughkeepsie, New York, USA, 12604

<sup>§</sup>Corresponding author

Email addresses:

ST: [stian@rockefeller.edu](mailto:stian@rockefeller.edu)

CW: [chi.wang@uky.edu](mailto:chi.wang@uky.edu)

MWA: [mian@vassar.edu](mailto:mian@vassar.edu)

# Abstract

## Background

Non-small cell lung cancer (NSCLC) is the predominant histological type of lung cancer, accounting for up to 85% of cases. Disease stage is commonly used to determine adjuvant treatment eligibility of NSCLC patients, however, it is an imprecise predictor of the prognosis of an individual patient. Currently, many researchers resort to microarray technology for identifying relevant genetic prognostic markers, with particular attention on trimming or extending a Cox regression model.

Among NSCLC, adenocarcinoma (AC) and squamous cell carcinoma (SCC) are two major histology subtypes. It has been demonstrated that there exist fundamental differences in the underlying mechanisms between them, which motivated us to postulate there might exist specific genes relevant to prognosis of each histology subtype.

## Results

In this article, we propose a simple filterer feature selection algorithm with a Cox regression model as the base. Applying this method to a real-world microarray data, no evidence has been found to support the existence of histology-specific prognostic gene signature. Nevertheless, a 31-gene prognostic gene signature for the early-stage AC and SCC samples is obtained, which provides comparable performance when compared with other relevant signatures.

## Conclusions

Our proposal is conceptually simple and straightforward to implement. Therefore, it is expected that other researchers, especially those with less statistical knowledge and experience, can adapt this method readily to test their own research hypotheses.

## Keywords:

Non-small cell lung cancer (NSCLC); adenocarcinoma (AC); squamous cell carcinoma (SCC); Cox model; prognosis; histology-subtype specific; gene expression barcode; feature selection algorithm.

## Background

Non-small cell lung cancer (NSCLC) is the predominant histological type of lung cancer, accounting for up to 85% of cases [1]. The overall five-year survival rate of NSCLC was estimated extremely low at a rate of roughly 15% due to late discovery of disease among more than two-thirds of NSCLC patients, for whom surgical resection is no longer an option [2]. Moreover, even among early stage subjects who had surgery, roughly 50% would have and then die of tumor recurrence [3]. Clinical studies [4, 5] have demonstrated that adjuvant chemotherapy significantly improved the survival of NSCLC patients at early stages. Disease stage is commonly used to determine adjuvant treatment eligibility, however, it is quite possible that a proportion of stage I subjects have poorer prognosis and may benefit significantly from adjuvant chemotherapy while some relatively good prognosis stage II subjects may not benefit significantly from adjuvant chemotherapies. Therefore, identification of poor prognosis of early stage NSCLC patients will assist in the prescription and administration of additional therapeutic intervention, which potentially leads to better survival for those patients.

Microarray technology allows simultaneous monitoring and measuring of tens of thousands of gene expression. Its important applications include current heating interest in relating gene expression profiles to survival phenotypes such as time to cancer recurrence or death. When analyzing data from a microarray experiment, a feature selection algorithm is usually considered to tackle with difficulties associated with the problem of the number of covariates being much larger compared with the number of samples, and to define a relevant gene subset informative about the underlying differences among different phenotypes. Based on how the model fitting is combined with the relevant subset selection, a feature selection algorithm can be categorized into three types, i.e., filterer, embedded and wrapper [6]. Table 1 in [6] summarizes these feature selection types plus their pros and cons and provides typical examples.

With regard to survival analysis using microarray data, prevalent attention has focused on trimming or extending the Cox regression model [7] to identify relevant genes associated with survival phenotypes because of its popularity in the analysis of survival data from traditional clinical settings. For instance, Gui and Li [8] proposed a novel feature selection algorithm called *LARS-cox*, which uses the least angle regressions (LARS) algorithm to obtain the solutions for the Cox model with L1 penalty. In a L1 penalty model, also referred to as the least absolute shrinkage and selection operator (Lasso) model, the negative log partial likelihood subject to the sum of the absolute value of the coefficients being less than a constant  $s$  is the objective function being minimized. However, several investigators have criticized LARS-cox for computational complexity and instability based on the fact that it needs to calculate inversion of high-dimensional matrices. As a solution to this problem, Sohn et al [9] apply the gradient lasso algorithm to a Cox model with L1 penalty instead and claim the proposed method has better stability, saves computing time, and achieves the global optimum. This algorithm was named *glcoxph*.

Among NSCLC, adenocarcinoma (AC) and squamous cell carcinoma (SCC), each approximately accounting for 40% of NSCLC cases, are two major histology subtypes. It has been well demonstrated that there exists fundamental differences in the underlying mechanisms of tumor development, growth, and invasion between the two subtypes [6,7]. Therefore, successful classification of NSCLC patients into their corresponding subtypes is of clinical importance as well. So far, many efforts [11–14] have been devoted to highlight those subtype-specific genes aimed at a precise diagnosis of NSCLC subtype and a feasible guide for personalized medicine. In those studies, a novel feature selection algorithm is usually adapted and utilized. Such fundamental differences between AC and SCC of NSCLC patients motivated us to speculate that there exist specific genes related to survival rates uniquely for each

histology subtype. To the best of our knowledge, however, all proposed Cox-model extensions ignore the phenotype histology subtype information because their main objective is to discriminate patients into subgroups with different survival rates based on gene expression data, meaning selection of meaningful gene subsets associated with prognosis for the whole set regardless of specific subpopulation characteristics.

In this article, we propose a simple filterer feature selection algorithm with a Cox regression model as the foundation. In addition, the expression barcode values [15, 16] instead of the actual expression values are proposed to be used, which eliminates genes with weak association. Such genes tend to be noise with high probabilities. Our focus is set on identification of separate gene subsets that can explain the difference in survival rates of AC and SCC among NSCLC patients. Compared to an embedded feature selection method such as *LARS-cox* and *glcoxph*, our proposal is conceptually simple and straightforward to implement. Moreover, those methods cannot identify the desired gene sets unless they are extended for such purpose. Such extensions are non-trivial. Therefore, it is expected that other researchers, especially those with less statistical knowledge and experience, can adapt this method readily to test their research hypotheses.

## Methods and Material

### The Experimental Data

The lung cancer microarray experiment under consideration was conducted by [17], with an objective of assessing the appropriateness and accuracy of their previously constructed 15-gene prognostic signature from another independent NSCLC microarray experiment [18].

This study had been deposited in Gene Expression Omnibus (GEO) repository under the accession number of GSE50081. It was hybridized on Affymetrix HGU133 Plus 2.0 chips and there were 181 samples in the original raw data. Since here we were only interested in AC and SCC subtypes, we excluded those samples with ambiguous histology subtype labels or histology subtypes other than AC and SCC, resulting in 127 AC and 42 SCC samples in our analysis, respectively.

### Pre-processing procedures

The raw Affymetrix data (CEL files) and patients' clinical profiles such as survival time, age, histology subtype, and smoking status were downloaded from the GEO repository and expression values were obtained using the *GCRMA* [19] algorithm. Data normalization across samples was carried out using quantile normalization and the resulting expression values were  $\log_2$  transformed.

First, only those probe sets that demonstrated a certain degree of variation across samples in each study were selected. Probe sets with SD below 0.1 were regarded as non-informative and eliminated. Then moderated t-tests using *limma* [20] were conducted to identify the differentially expressed genes (DEGs) between SCC and AC. Exclusion of those non-DEGs served as the second step of the filtering, and the cutoff for the false discovery rate (FDR) was set at 0.05. There were 5465 down- and 5484 up-regulated probe sets, corresponding to 6202 unique DEGs.

When using the barcoded values, the probe sets expressed at extremely high (>95% in AC and >90% in SCC) or low frequencies (<5% in AC and <10% in SCC) were eliminated. This additional exclusion is necessary to avoid the fitting problems associated with complete separation, e.g., for one specific gene all SCC samples are expressed while silenced in AC samples. Notably, we chose the different cutoffs for

AC and SCC, mainly because the number of SCC samples is only one third that of AC samples. To deal with multiple probe sets matched to one specific gene, the one with the largest fold change was kept. The resulting 2207 probe sets corresponding to 1889 unique DEGs were fed into the downstream analysis.

## Methods

### *The Cox proportional model to identify subtype-survival relevant genes*

To identify those genes informative to both AC/SCC histology subtype and survival rate, a Cox model is utilized for each gene. Specifically, for patient  $i$  ( $i=1, \dots, N_j$ ) of subtype  $j$  ( $j=0, 1$  representing AC and SCC, respectively),  $t_{ij}$ ,  $\delta_{ij}$ ,  $x_{ij1}, \dots, x_{ijp}$  are observed. Here,  $\delta_{ij}$  is the censoring indicator taking 1 if this patient is dead and 0 otherwise,  $t_{ij}$  denotes survival time if  $\delta_{ij}=1$  or censoring time otherwise, and  $x_{ij}=(x_{ij1}, \dots, x_{ijp})^T$  is the vector of actual expression values or the barcoded expression values for  $p$  genes. Then the hazard function of this patient for gene  $g$  ( $g=1, \dots, p$ ) is as follows:

$$\lambda_{ijg}(t) = \lambda_{0g}(t) \exp(\beta_{1g} I(j=1) + \beta_{2g} X_{ijg} + \beta_{3g} I(j=1) \times X_{ijg}) \quad (1)$$

where  $\lambda_{0g}(t)$  is an unknown baseline hazard function and  $I(j=1)$  is the indicator being 1 if the histology subtype of the patient  $j$  belongs to SCC and 0 otherwise. Here,  $\beta_{2g}$  and  $\beta_{3g}$  are the parameters of interest, with  $\beta_{2g}$  representing the change in hazard rate if the actual expression value of gene  $g$  increases by one unit or gene  $g$  is expressed for the AC subtype and  $\beta_{3g}$  representing extra change in such a hazard rate for being a SCC subtype. Particularly, only when the subsets of  $\beta_{2g}$  and  $\beta_{2g} + \beta_{3g}$  being statistically different from zeros are mutually exclusive implied no overlap between histology-specific prognostic genes. Figure 1 illustrated all possible scenarios.

It is worth mentioning that  $\lambda_{0g}$  and  $\beta_{1g}$  are gene-specific, i.e. the subscript  $g$  cannot be dropped. Consequently, the influence of other relevant genes other than the specific gene  $g$  and clinical covariates, and of imbalance among those covariates in between AC and SCC subtypes, can be taken into account. Moreover, we followed the statement given by [17] that “patients with more than 5 years follow-up were censored at 5 years as deaths occurring later than 5 years were not likely to be lung cancer related”, and used overall survival up to 5 years as the endpoint of interest. Therefore, a patient with a longer-than-5 survival time was censored at year 5. To correct for multiple comparison, Benjamini and Hochberg procedure [21] was used.

### *Barcode algorithm*

In the barcode algorithm, the expressed genes are coded with ones and the silenced genes are coded with zeros. Briefly, McCall et al [16] used a mixture model to fit the silenced and expressed distribution of observed  $\log_2$  transformed intensity values for each gene. The mathematical notation for this model is as following,

$$\begin{aligned} y_{ig} | \mu_g &\sim (1 - p_g) \times N(\mu_g, \tau_g^2) + p_g \times U(\mu_g, S_g) \\ \mu_g &\sim N(\xi, \lambda^2) \\ \tau_g^2 &\sim IG(\alpha, \beta) \end{aligned}$$

where  $y_{ig}$  is the observed  $\log_2$  intensity for gene  $g$  in sample  $i$ , and it is assumed that  $y_{ig}$  follows a mixture of a silenced normal distribution of  $N(\mu_g, \tau_g^2)$ , and an expressed uniform distribution of  $U(\mu_g,$

$S_g$ ) from the silenced mean to a saturation value represented by  $S_g$ . Lastly, a parametric distribution is specified for the silenced means and variances for each gene, one coming from a normal distribution while the other from an inverse gamma distribution. By introducing higher-level parameters, i.e.,  $\alpha$ ,  $\beta$ ,  $\xi$ , and  $\lambda$ , more stable estimates of  $\tau_g^2$  can be obtained because the information would be borrowed and shared across genes, leading to a shrinkage of individual estimate toward the overall average, in a hierarchical model.

To know whether the observed  $\log_2$  expression value  $y_{ig}$  is more likely to come from the silenced distribution or the expressed distribution, standardized intensity value, i.e.,  $(y_{ig} - \mu_g) / \tau_g$ , which follows a standard normal distribution under the null hypothesis was calculated. Using a hard-threshold  $C$ , expression barcode for a gene, a vector of ones and zeros denoting which samples are expressed and silenced was coined,

$$b_{ig} = \begin{cases} 1 & \Phi(-(y_{ig} - \mu_g) / \tau_g) < C \\ 0 & \text{otherwise} \end{cases}$$

here  $\Phi$  is the cumulative density function of a standard normal. For the detailed description on how to estimate the parameters in the hierarchical model using EM algorithm, the supplementary material of [16] is referred.

#### **Statistical language and packages**

The statistical analysis including the survival analysis was carried out in the R language version 3.0 ([www.r-project.org](http://www.r-project.org)), and packages such as *frma* (for barcode) and *gcrma* were from the Bioconductor project ([www.bioconductor.org](http://www.bioconductor.org)).

## **Results and Discussion**

### **Real data**

As mentioned in the **Introduction** section, the existence of a small subset of genes specifically relevant to both different histology subtypes and survival rates is desired. We applied the filter feature selection method introduced in the **Methods** section to test this research hypothesis. Unexpectedly, there is no evidence to support the existence of such specific subsets instead. Figure 2 highlights the study schema.

### **Feature selection using Cox models**

First, the Cox model in Equation 1 was fit and the parameters of interest were estimated for each gene under consideration. Based on the actual expression values without extra barcode frequency filtering, there are 239 and 0 gene whose second and third coefficients, respectively, were statistically significantly different from zero. With extra barcode frequency filtering, there are 144 genes and 0 genes with second and third coefficients, respectively, statistically significantly different from zero upon the actual expression values while there are 31 genes and 0 gene respectively upon the barcode expression values. The Venn-diagram showing how these three selected gene sets overlapped is presented in Figure 3.

We found no evidence to support the existence of histology-specific prognostic genes, since none of the interaction terms was statistically significant, regardless of which gene expression values were being used. We did observe, however, that the number of prognostic genes for NSCLC early stages tends to be

bigger using the actual expression values compared to using the barcoded values. One possible explanation for this pattern is that after the actual expression values were dichotomized into barcoded values, the genes with weak or even moderate association to survival rate were discarded.

### ***Risk score construction***

Given that the number of selected genes is large, especially when the actual expression values are used, a regression model including all selected genes as covariates is impossible. Instead, we adapt the procedure in [18] and modify it to construct a risk score for each individual in this study. This procedure consists of two steps. As the first step, a principal component analysis (PCA) is conducted and the first four principal components (PCs) are recorded. Then a multiple Cox regression model with the first four PCs as covariates is fitted, the risk scores are calculated with the coefficients of these four PCs in the Cox model serving as the weights. As a modification, the number of PCs is determined by the proportion of variance in those selected genes explained by PCs, with the threshold being set at 70%. Moreover, since PCA is only applicable for continuous variables, the actual expression values of 31-gene identified using barcode values were used when estimating risk scores to evaluate the performance of this signature.

Using the mean value of those risk scores as a cutoff, the patients were classified into either a low-risk group or a high-risk group. The Kaplan-Meier curve using the resulting risk scores was drawn and the p-value from a log rank test that compares these two profiles was provided. Also, after excluding those censored before 5-year, the samples were divided into two groups based on their status on 5-year survival. The classification *accuracy* and the area under ROC curve (AUC) statistics were computed. The results were tabulated in Table 1, and the Kaplan-Meier curves were presented in Figure 4.

### ***Comparison with relevant prognostic signatures***

Although the clinical-pathological staging is currently the standard of determining NSCLC prognosis, a number of gene expression signatures have been reported to have better performance of predicting survival in NSCLC patients. The article by Shao et al [22] provides a comprehensive review on those prognostic gene expression signatures.

Here, we compared our 31-gene signature with some of those signatures. Compared with the most relevant 15-gene signature, only the predictive rule constructed from using all 31 genes obtained from the data with barcode filtering as covariates established comparable performance with non-marginal but the least suffering (31 vs. 15) in parsimony (Table 2). Moreover, the 31-gene signature showed substantial superiority over the 13-gene signature given by Guo et al. [23]. Nevertheless, since the 31-gene signature was trained and tested on the same data set, additional validation of its significance on independent data is definitely desired.

Unsurprisingly, there is almost no overlap of genes between these signatures. As noted by many researchers [24, 25], the lack of consistency among gene expression signatures even using the same data is very common. This may be due to the noisy nature of microarray data, relatively small sample size of the study, and different preprocessing and downstream statistical methods used for data analysis. The examination on underlying pathways of those selected genes, aimed at exploring if those selected genes share the same pathways and thus act in concert among one another to have a meaningful biological effect, is a well-accepted alternative in the field [26]. The pathway enrichment analysis using STRING [27] is presented in the **additional file 1**.

Furthermore, we found that many genes in other signatures cannot survive our preprocessing filtering steps. There are two major objectives with preprocessing filtering. One is to exclude genes with high

probabilities of being irrelevant and thus to save on computing time. The other is to reduce the number of the genes under consideration, and thus to alleviate the multiple comparison problem and to avoid many false negatives. However, given that the appropriate choice of filtering may be data-specific, we cannot justify our filtering steps in a more general setting. A thorough investigation is warranted.

### Synthesized data

To explore the characteristics of our proposed procedure, thus to find a reasonable explanation to the negative results of our real data analysis, we used the actual expression values for 2207 probe-sets after barcode filtering to do the simulations. Here, we selected 4 genes as prognostic markers. The expression values of four genes, i.e., 224794\_s\_at, 201389\_at, 231094\_s\_at, 200827\_at were represented by  $X_1 \sim X_4$ , respectively.

**Extreme case 1: mutually exclusive markers for each subtype.** The hazard functions for AC and SCC are specified as follows,

$$\begin{aligned}\lambda_{SCC} &= \lambda_0 \exp(1.42X_1 - 0.75X_3) \\ \lambda_{AC} &= \lambda_0 \exp(0.225X_2 - 0.177X_4)\end{aligned}$$

Among the rest 2203 probe sets, we randomly selected 96 probe sets to make the number of features considered to 100. Thus, the features except gene 1-4 are random noises. The censoring rate was fixed at 30%, and this had been replicated for 50 times.

**Extreme case 2: no subtype specific prognostic genes at all.** Then we simulated other set of simulated data where both AC and SCC share the identical set of prognostic markers,

$$\lambda_{AC\&SCC} = \lambda_0 \exp(1.42X_1 - 0.75X_2 + 0.75X_3 - 0.59X_4)$$

then the proposed procedure was applied to these two synthesized data sets.

### Simulation Results

In extreme case 1, it is expected that at least  $\beta_2$ s for genes 3-4 and  $\beta_3$ s for genes 1-4 should have non-zero coefficients. The results are tabulated in Table 3A. However, we found out that when the signals are weak or moderate, indicating by the magnitudes of those linear coefficients associated with covariates, for SCC subtype,  $\beta_3$ s of genes 1-4 tend to be zeros (Data not shown). This implies that unless the signals are strong enough (like the coefficient of gene 1 in the simulation 1 for instance), the proposed procedure tends to miss the subtype-specific prognostic markers. It is suggested that the procedure might lack statistical power to detect the subtype-specific prognostic markers.

In extreme case 2, it is expected to only  $\beta_2$  for genes 1-4 have non-zero coefficients. As shown in Table 3B, the proposed procedure fulfilled this goal. Overall, when using the barcoded values, the total number of selected genes is substantially less than the number of using the actual values. This pattern has also been observed in the real data analysis. Additionally, the rate of false positives, as indicated by the average number of non-zero genes, is also high. Care is needed to eliminate the possible false positives.

### Conclusions

Based on the fundamental differences in the underlying mechanisms of tumor development, growth, and invasion between AC and SCC of NSCLC patients, we hypothesized that there might exist some specific genes relevant to survival rates uniquely for each of these two histology subtypes. Unexpectedly, there is

no evidence to support this conjecture when we applied a proposed filterer feature selection method to real-world microarray data.

This study has two major limitations. First, the data come from a single microarray experiment, thus the sample size is an issue. In particular, the number of SCC samples is 1/3 of the number of AC samples, which may cause imbalance between two histology subtypes. A larger data set that integrates many relevant microarray experiments but with careful handling on the batch effect is desired, whose results might be more statistically powerful and be generalized to a broader population. Second, the proposed feature selection method using Cox models to filter out the potential irrelevant genes might ignore the correlations and interactions among genes and cannot provide directly the overall prognostic effect of all selected genes combined together. Notably, the risk score construction is separated from the feature selection here.

As shown by the simulations, the Cox models proposed here tend to fail in identifying the significant interaction terms when such effects are not strong enough. Based on this, we cannot exclude the possibility that no evidence of existence in subtype-specific prognostic markers is due to weak or moderate signals of SCC markers. Currently, we are working on a new approach, which uses the partial likelihood and an embedded feature selection algorithm to select relevant genes and estimate risk scores simultaneously. Most importantly, it does not suffer from the above-mentioned disadvantages because it is essentially an embedded feature selection algorithm. Using a combined data set and this embedded feature selection method, the research hypothesis that the existence of histology-specific prognostic gene signatures will be tested again. The method will be presented in another paper.

Nevertheless, our proposal in this article has its own advantages. For instance, it is conceptually simple and straightforward to implement. Additionally, since it does not need to optimize tuning parameters via cross-validation and to estimate the corresponding coefficients for selected feature simultaneously on the training set, its saving on the computing time is obvious. Therefore, it is expected that other researchers, especially those with less statistical knowledge and experience, can adapt this method for their research purposes.

In conclusion, a research hypothesis has been generated and remains open for further testing. Hopefully, with the method proposed in this study as a spark, more relevant and novel feature selection algorithms will be conceived and developed. Only then is the correct answer to this research question possible to be unveiled.

## Abbreviations

NSCLC: non-small cell lung cancer; AC: adenocarcinoma; SCC: squamous cell carcinoma; PCA: principal component analysis; FDR: false discovery rate; GEO: Gene Expression Omnibus; DEG: differentially expressed gene; LARS: least angle regressions.

## Competing interests

No competing interests have been declared.

## Authors' Contributions

Conceived and designed the study: ST. Analyzed the data: ST CW MWA. Interpreted data analysis and results: ST MWA CW. Wrote the paper: ST CW MWA. All authors reviewed and approved the final manuscript.

## Acknowledgements

The study was supported by a seed fund from the Jilin University (No 450060491885). We thank Drs. Chang-Qi Zhu and Ming-Sound Tsao for the assistance on GSE50081 data retrieval and Ms. Tianjiao Wang for the data retrieval.

## References:

1. Yang P, Allen MS, Aubry MC, Wampfler JA, Marks RS, Edell ES, Thibodeau S, Adjei AA, Jett J, Deschamps C: **Clinical features of 5,628 primary lung cancer patients: experience at Mayo Clinic from 1997 to 2003.** *Chest* 2005, **128**:452–462.
2. Siegel R, Ward E, Brawley O, Jemal A: **Cancer statistics, 2011.** *CA Cancer J Clin* 2011, **61**:212–236.
3. Lu Y, Lemon W, Liu P-Y, Yi Y, Morrison C, Yang P, Sun Z, Szoke J, Gerald WL, Watson M, Govindan R, You M: **A gene expression signature predicts survival of patients with stage I non-small cell lung cancer.** *PLoS Med* 2006, **3**:e467.
4. Visbal AL, Leighl NB, Feld R, Shepherd FA: **Adjuvant Chemotherapy for Early-Stage Non-small Cell Lung Cancer.** *Chest* 2005, **128**:2933–2943.
5. Winton T, Livingston R, Johnson D, Rigas J, Johnston M, Butts C, Cormier Y, Goss G, Inculet R, Vallieres E, Fry W, Bethune D, Ayoub J, Ding K, Seymour L, Graham B, Tsao M-S, Gandara D, Kesler K, Demmy T, Shepherd F: *Vinorelbine plus cisplatin vs. observation in resected non-small-cell lung cancer.* 2005, **352**:2589–2597.
6. Saeys Y, Inza I, Larrañaga P: **A review of feature selection techniques in bioinformatics.** *Bioinformatics* 2007, **23**:2507–17.
7. Cox DR: **Regression models and life-tables.** *J R Stat Soc B* 1972, **34**:187–220.
8. Gui J, Li H: **Penalized Cox regression analysis in the high-dimensional and low-sample size settings, with applications to microarray gene expression data.** *Bioinformatics* 2005, **21**:3001–8.
9. Sohn I, Kim J, Jung S-H, Park C: **Gradient lasso for Cox proportional hazards model.** *Bioinformatics* 2009, **25**:1775–81.
10. Kikuchi T, Daigo Y, Katagiri T, Tsunoda T, Okada K, Kakiuchi S, Zembutsu H, Furukawa Y, Kawamura M, Kobayashi K, Imai K, Nakamura Y: **Expression profiles of non-small cell lung cancers on cDNA microarrays: identification of genes for prediction of lymph-node metastasis and sensitivity to anti-cancer drugs.** *Oncogene* 2003, **22**:2192–205.

11. Sanchez-Palencia A, Gomez-Morales M, Gomez-Capilla JA, Pedraza V, Boyero L, Rosell R, Fárez-Vidal ME: **Gene expression profiling reveals novel biomarkers in nonsmall cell lung cancer.** *Int J Cancer* 2011, **129**:355–64.
12. Tian S, Suárez-fariñas M: **Hierarchical-TGDR: Combining biological hierarchy with a regularization method for multi-class classification of lung cancer samples via high-throughput gene-expression data.** *Syst Biomed* 2013, **1**:93–102.
13. Ben-hamo R, Boue S, Martin F, Talikka M, Efroni S: **Classification of lung adenocarcinoma and squamous cell carcinoma samples based on their gene expression profile in the sbv IMPROVER Diagnostic Signature Challenge.** *Syst Biomed* 2013:83–92.
14. Mramor M, Leban G, Demsar J, Zupan B: **Visualization-based cancer microarray data classification analysis.** *Bioinformatics* 2007, **23**:2147–54.
15. Zilliox MJ, Irizarry RA: **A gene expression bar code for microarray data.** *Nat Methods* 2007, **4**:911–913.
16. McCall MN, Uppal K, Jaffee HA, Zilliox MJ, Irizarry RA: **The gene expression barcode: Leveraging public data repositories to begin cataloging the human and murine transcriptomes.** *Nucleic Acids Res* 2011, **39**:D1011–D1015.
17. Der SD, Sykes J, Pintilie M, Zhu C, Strumpf D, Liu N, Jurisica I, Shepherd FA, Tsao M-S: **Validation of a Histology-Independent Prognostic Gene Including Stage IA Patients.** *J Thorac Oncol* 2014, **9**:59–64.
18. Zhu C-Q, Ding K, Strumpf D, Weir BA, Meyerson M, Pennell N, Thomas RK, Naoki K, Ladd-Acosta C, Liu N, Pintilie M, Der S, Seymour L, Jurisica I, Shepherd FA, Tsao M-S: **Prognostic and predictive gene signature for adjuvant chemotherapy in resected non-small-cell lung cancer.** *J Clin Oncol* 2010, **28**:4417–4424.
19. Wu Z, Irizarry RA, Gentleman R, Martinez-Murillo F, Spencer F: **A Model-Based Background Adjustment for Oligonucleotide Expression Arrays.** *J Am Stat Assoc* 2004, **99**:909–917.
20. Smyth G: **Limma: linear models for microarray data.** In ... *Comput Biol Solut using R* .... edited by R. Gentleman, V. Carey, S. Dudoit, R. Irizarry WH (eds. . New York: Springer; 2005:397–420.
21. Benjamini Y, Hochberg Y: **Controlling the False Discovery Rate: A Practical and Powerful Approach to Multiple Testing.** *J R Stat Soc Ser B* 1995, **57**:289 – 300.
22. Shao W, Wang D, He J: **The role of gene expression profiling in early-stage non-small cell lung cancer.** *J Thorac Dis* 2010, **2**:89–99.
23. Guo N, Wan Y, Bose S: **A novel network model identified a 13-gene lung cancer prognostic signature.** *Int J ...* 2011, **4**:19–39.
24. Ein-Dor L, Kela I, Getz G, Givol D, Domany E: **Outcome signature genes in breast cancer: is there a unique set?** *Bioinformatics* 2005, **21**:171–8.

25. Tan PK, Downey TJ, Spitznagel EL, Xu P, Fu D, Dimitrov DS, Lempicki RA, Raaka BM, Cam MC: **Evaluation of gene expression measurements from commercial microarray platforms.** *Nucleic Acids Res* 2003, **31**:5676–5684.

26. Manoli T, Gretz N, Gröne H-J, Kenzelmann M, Eils R, Brors B: **Group testing for pathway analysis improves comparability of different microarray datasets.** *Bioinformatics* 2006, **22**:2500–6.

27. Franceschini A, Szklarczyk D, Frankild S, Kuhn M, Simonovic M, Roth A, Lin J, Minguez P, Bork P, von Mering C, Jensen LJ: **STRING v9.1: protein-protein interaction networks, with increased coverage and integration.** *Nucleic Acids Res* 2013, **41**:D808–15.

## Tables

**Table 1. The performance of different gene signatures**

Signature	# low /high risk	# of PCs/ % of variance explained	Accuracy (%)	AUC (%)	p-value (log rank)
A: using the modified PCA procedure for risk score construction					
239-gene	92/77	1/77.79%	60.45	61.82	$6.14 \times 10^{-3}$
144-gene	74/95	7/70.95%	61.94	<b>71.90</b>	$9.21 \times 10^{-4}$
31-gene	78/91	5/73.48%	66.42	70.63	<b><math>2.34 \times 10^{-5}</math></b>
15-gene by Zhu	97/72	4/74.15%	<b>67.16</b>	70.72	$4.88 \times 10^{-4}$
13-gene by Guo	96/73	4/70.22%	55.97	59.82	$1.16 \times 10^{-1}$
B: using all covariates in the cox model for risk score construction					
<b>31-gene actual</b>	<b>88/81</b>	--	<b>74.63</b>	<b>79.68</b>	<b><math>9.70 \times 10^{-9}</math></b>
31-gene barcode	89/80	--	70.90	78.95	$8.33 \times 10^{-7}$
15-gene actual	86/83	--	67.16	73.81	$3.32 \times 10^{-5}$
13-gene actual	86/83	--	58.96	65.66	$5.32 \times 10^{-3}$

**Table 2. The 31-gene signature**

Probe set	Symbol	$\beta_{\text{barcode}}$	$\beta_{\text{actual}}$
214033_at	ABCC6	0.8396	0.0324
228241_at	AGR3	-0.5039	-0.0825
219366_at	AVEN	0.6165	0.3339
223623_at	C2orf40	-0.6727	-0.2181
219572_at	CADPS2	0.4376	0.0461
204995_at	CDK5R1	-0.3820	-0.1851
224794_s_at	CERCAM	1.6911	1.4224
52255_s_at	COL5A3	0.1711	0.1734
205399_at	DCLK1	-0.2630	-0.0908
203698_s_at	FRZB	-0.5041	-0.1230
223423_at	GPR160	0.2560	-0.2284
201389_at	ITGA5	-0.7545	-0.7546
228564_at	LOC375295	0.0486	-0.1917
202828_s_at	MMP14	-0.3379	-0.3097
231094_s_at	MTHFD1L	0.7513	0.7506
229659_s_at	PIGR	0.2571	0.1112
200827_at	PLOD1	-0.2642	-0.5879
219127_at	PRR15L	-0.5165	-0.0160
202937_x_at	RRP7A	-0.1779	-0.0854
229910_at	SHE	0.5167	0.0349
200711_s_at	SKP1	-0.4436	0.0581
232432_s_at	SLC30A5	-1.0383	-0.3597
228951_at	SLC38A7	-0.1447	-0.1182
205597_at	SLC44A4	0.2840	0.1099
213508_at	SPTSSA	0.1383	0.1421
226388_at	TCEA3	-1.0810	-0.0657
204529_s_at	TOX	-0.6527	-0.4013
216623_x_at	TOX3	-0.0875	-0.0153
203824_at	TSPAN8	-0.5017	0.0479
202749_at	WRB	-0.2680	0.0641
212774_at	ZBTB18	0.2709	0.2569

**Table 3. The simulation results**

	Actual value (frequency %)		Barcoded value (frequency %)	
	$\beta_2$	$\beta_3$	$\beta_2$	$\beta_3$
<b>A. Simulation 1</b>				
Gene1	100	100	100	94
Gene2	100	0	100	0
Gene3	100	100	100	86
Gene4	100	100	100	16
Ave.# of non-zero genes	55.68	19.8	39.92	14.04
<b>B. Simulation 2</b>				
Gene1	100	0	100	0
Gene2	100	0	100	0
Gene3	100	0	100	0
Gene4	100	0	100	0
Ave.# of non-zero genes	45.7	0.2	28.9	0.22

## Figures

Figure 1. The Scenarios of the cox model and their interpretation

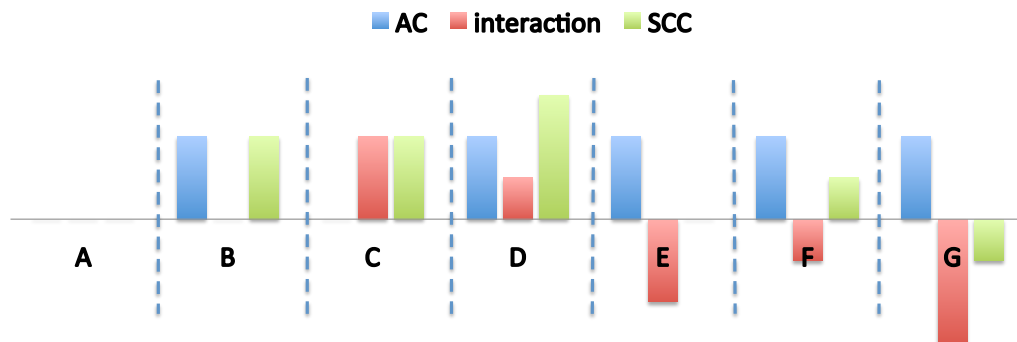
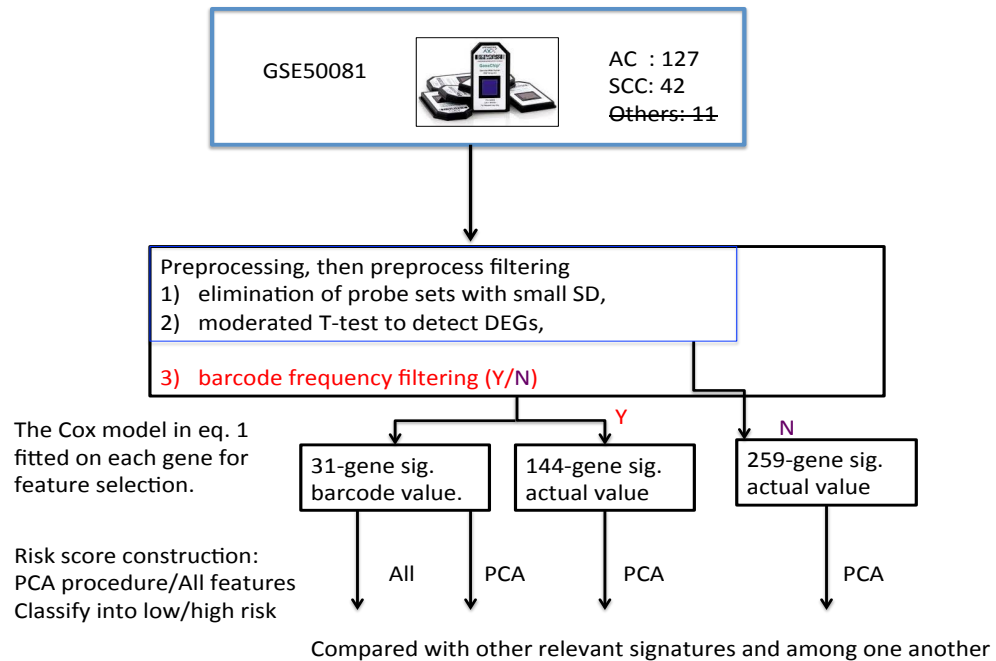


Table: The interpretation of every scenario

Case	Condition	Extra condition	Interpretation
A	$\beta_2=0, \beta_3=0$	--	Not a prognostic marker
B	$\beta_2 \neq 0, \beta_3=0$	--	Overall prognostic marker, no AC/SCC specific genes
C	$\beta_3 \neq 0, \beta_2=0$	--	SCC specific prognostic marker
D	$\beta_2 \neq 0, \beta_3 \neq 0$	$\beta_2 \times \beta_3 > 0$	Prognostic marker for both AC and SCC specific, the magnitude increases.
E	$\beta_2 \neq 0, \beta_3 \neq 0$	$\beta_2 + \beta_3 = 0$	AC specific prognostic marker
F	$\beta_2 \neq 0, \beta_3 \neq 0$	$\beta_2 \times \beta_3 < 0,  \beta_2  >  \beta_3 $	Both AC and SCC specific gene, the magnitude decreases.
G	$\beta_2 \neq 0, \beta_3 \neq 0$	$\beta_2 \times \beta_3 < 0,  \beta_2  <  \beta_3 $	Both AC and SCC specific gene, the direction changes.

**Figure 2. The study schema**



**Figure 3. The Venn-diagram**

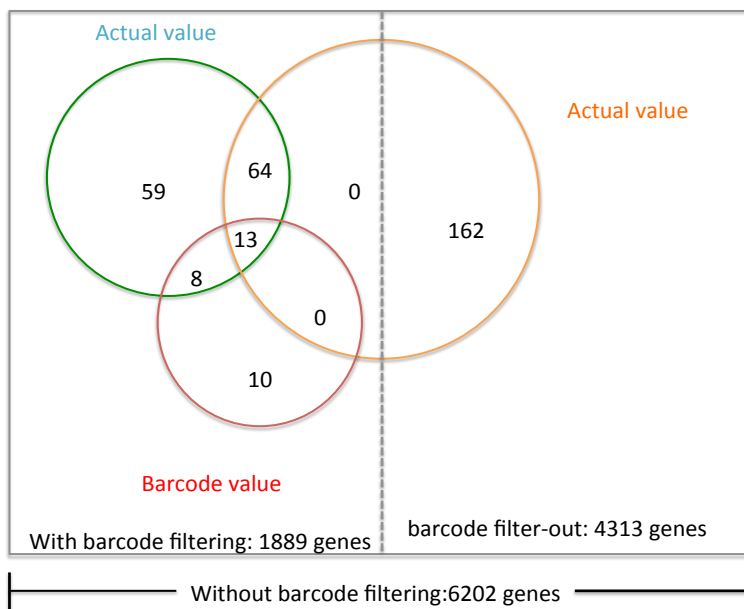
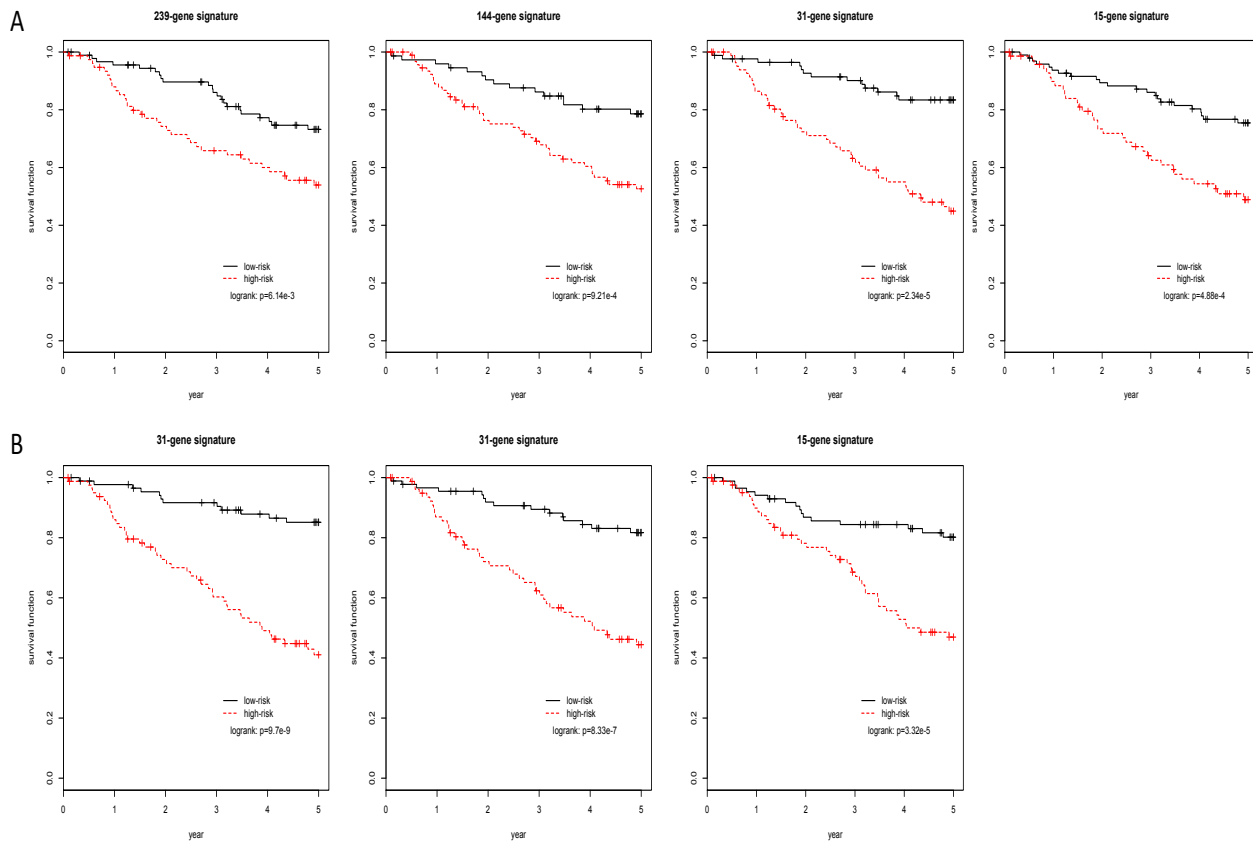


**Figure 4. The Kaplan-Meier curves between high-risk and low-risk groups using different prognostic signatures**



## Additional files

### Additional file 1-Supplementary materials: functional protein-protein network analysis

To explore the possible relationship of the 31-gene signature with other relevant prognostic signatures, the functional protein-protein interaction network using an online database called STRING (<http://www.string-db.org>) had been conducted. The possible interacted functional proteins with those identified in three signatures were shown in Supp. Figure 1.

Using the KEGG pathways enrichment analysis inside STRING, the top enrichment pathways for each signature were presented in Supp. Table 1. The only overlapped enriched pathway is cell cycle between our 31-gene signature and the 15-gene signature. The numbers of significant GO terms for those signatures were 44 for 31-gene signature, 38 for 15-gene signature, and 51 for 12-gene signature, respectively. Unfortunately, there was no overlap among those GO-terms at all. There were 1, 0, 2 overlaps between 15-gene, 12-gene and 31-gene signature pairwise. To conclude, there is a long way to go before a biologically meaningful prognostic signature for non-small cell lung cancer can be put into practice in a clinical setting.

**Supp. Table1. The enriched KEGG pathways in those signatures**

A. Enriched KEGG pathways in our 31-gene signature				
ID	Pathway	# Genes	p-value	p-value_fdr
hsa04710	Circadian rhythm - mammal	5	5.70E-09	1.35E-06
hsa04120	Ubiquitin mediated proteolysis	7	1.22E-07	1.45E-05
hsa04512	ECM-receptor interaction	5	6.24E-06	4.93E-04
hsa04114	Oocyte meiosis	5	1.93E-05	1.14E-03
hsa05131	Shigellosis	4	3.03E-05	1.44E-03
hsa04310	Wnt signaling pathway	5	8.94E-05	3.53E-03
hsa04510	Focal adhesion	5	3.46E-04	1.17E-02
<b>hsa04110</b>	<b>Cell cycle</b>	<b>4</b>	<b>5.52E-04</b>	<b>1.63E-02</b>
hsa05100	Bacterial invasion of epithelial cells	3	1.29E-03	3.39E-02
B. Enriched KEGG pathways in 15-gene signature by Der et al, 2014				
hsa05214	Glioma	4	5.36E-06	6.95E-04
hsa05218	Melanoma	4	8.79E-06	6.95E-04
hsa05220	Chronic myeloid leukemia	4	8.79E-06	6.95E-04
hsa05215	Prostate cancer	4	2.22E-05	1.31E-03
hsa05219	Bladder cancer	3	6.60E-05	3.13E-03
hsa05223	Non-small cell lung cancer	3	1.46E-04	5.75E-03
hsa05212	Pancreatic cancer	3	2.70E-04	8.78E-03
hsa04115	p53 signaling pathway	3	2.96E-04	8.78E-03
hsa05222	Small cell lung cancer	3	6.25E-04	1.65E-02
<b>hsa04110</b>	<b>Cell cycle</b>	<b>3</b>	<b>1.71E-03</b>	<b>4.04E-02</b>
C. Enriched KEGG pathways in 15-gene signature by Guo et al, 2011				
hsa05164	Influenza A	6	8.02E-07	1.90E-04
hsa05160	Hepatitis C	5	5.90E-06	5.30E-04
hsa04623	Cytosolic DNA-sensing pathway	4	6.71E-06	5.30E-04
hsa04622	RIG-I-like receptor signaling pathway	4	1.26E-05	7.46E-04
hsa04620	Toll-like receptor signaling pathway	4	5.28E-05	2.50E-03
hsa05162	Measles	4	1.53E-04	6.00E-03
hsa04150	mTOR signaling pathway	3	1.77E-04	6.00E-03
hsa04720	Long-term potentiation	3	4.00E-04	1.18E-02
hsa05215	Prostate cancer	3	8.61E-04	2.27E-02
hsa04916	Melanogenesis	3	1.18E-03	2.80E-02

**Supp. Figure 1. The functional protein-protein networks for three signatures**

